PHILOSOPHICAL TRANSACTIONS OF THE ROYAL SOCIETY A MATHEMATICAL, PHYSICAL & ENGINEERING SCIENCES

Deformation microstructures and textures in steels

Bevis Hutchinson

Phil. Trans. R. Soc. Lond. A 1999 **357**, 1471-1485
doi: 10.1098/rsta.1999.0385

THE ROYAL SOCIETY

Deformation microstructures and textures in steels

By Bevis Hutchinson

Swedish Institute for Metals Research, Drottning Kristinas väg 48, S-114 28 Stockholm, Sweden

Experimental evidence concerning the evolution of textures and substructures during cold rolling of low-carbon steel is presented and reviewed with some reference to the importance of these during subsequent annealing. Attention is paid to the orientation dependence of microstructure and stored energy of deformation. These are considered in relation to the Taylor factors for grains of different orientations in homogeneous deformation, and to the occurrence of different types of heterogeneity. Certain grain-scale heterogeneities appear to be important in defining the textures, which can now be predicted with some success using so-called relaxed constraint models. Intragranular heterogeneities also play a role and these especially affect the variation in substructure between grains. The strain-rate sensitivity of flow stress is an important parameter, which, depending on its sign and magnitude, may cause either severe strain localization in shear bands or lead to very homogeneous deformation structures where the influence of crystal orientation almost disappears.

Keywords: steel; deformation; texture; microstructure

1. Introduction

Studies of deformation substructures in steels have mostly been motivated by a desire to understand better the recrystallization behaviour and texture evolution in cold-rolled and annealed sheets. The present review will also be concentrated with these aspects in mind. For completeness, we will also point out that some important studies of work hardening have also concerned steels (see, for example, Langford & Cohen 1969; Roven & Nes 1984; Jago & Hansen 1986). There are, however, surprisingly few detailed examinations of the evolution of deformation substructures in iron or low-carbon steels, in contrast to the case of FCC metals such as aluminium, copper or nickel (Hansen & Hughes 1995).

During industrial production, steel sheet is normally cold rolled between 50% and 90% reduction prior to annealing with the intention of producing a final grain structure and texture suitable for cold forming of products such as automotive panels. In particular, it is desirable to develop a spread of orientations with {111} planes parallel to the sheet, the so-called γ-fibre texture. Many factors are known to influence the strength of the final γ-fibre texture; some seem to operate through their action on the recovery and recrystallization processes during annealing, while others control the initial structure that results from cold rolling. Table 1 is an attempt to assign responsibility to some of these factors and it is evident that several of these principally affect the material in its cold-rolled state. This is, therefore, a practical reason for wanting to know more about deformation structures in steels. Furthermore, it is

Table 1. *Factors affecting the annealing textures of steels via their effects on deformation and recrystallization processes*

factor controlling γ-fibre texture	during cold rolling	during annealing (recrystallization)
cold rolling reduction	deformation texture sharpness and substructure density	—
temperature of rolling	homogeneity of deformation	—
initial grain size	number and types of sites for nucleation	—
coarse second phases (e.g. cementite particles)	deformation zones as nucleation sites	—
fine second phases (e.g. AlN)	—	preferential inhibition of nucleation
interstitial elements (carbon, nitrogen)	homogeneity of deformation	interference with nucleation and growth
substitutional elements (e.g. manganese)	—	inhibition of growth

now evident (see, for example, Dillamore *et al*. 1967; Every & Hatherly 1974; Kern 1984; Inagaki 1994; Vanderscheuren *et al*. 1996) that dislocation substructures have a close relationship with the orientation of the cold-rolled grain, and so the structures resulting from deformation must always be considered together with the deformation textures.

2. Rolling textures

In BCC metals such as ferritic steels, the cold rolling textures are rather insensitive to material and process parameters. The degree of deformation (rolling reduction) is important for the texture sharpness and for the relative strength of different components. The latter is also affected by the presence of a starting texture, but other parameters such as grain size and rolling pass schedule have little influence, provided that surface friction effects do not become significant. There are some subtle effects of deformation homogeneity that can be detected in the sharpness of the texture, and we shall return to these subsequently as they can have important consequences.

The evolution of texture in steel with increasing rolling reduction has been examined in numerous investigations using the orientation distribution function (ODF) technique (see, for example, Heckler & Granzow 1970; Schläfer & Bunge 1974; von Schlippenbach *et al*. 1986; Inagaki 1987). The present discussion is based on neutron diffraction results of Schläfer & Bunge (1974), which have subsequently been corrected for 'ghost effects'. Figure 1 shows sections of the orientation distribution function with $\phi_2 = 45°$, which includes almost all the important components in rolled steels. The textures after 50%, 74% and 95% reduction (true strains of 0.69, 1.43 and 3.0) are shown in figure 1*a*–*c* while figure 1*d* shows a key to the main orientations. In all cases, the textures are concentrated into two families, the α-fibre with $\langle 110 \rangle$ parallel to the rolling direction and the γ-fibre with $\langle 111 \rangle$ along the normal direc-

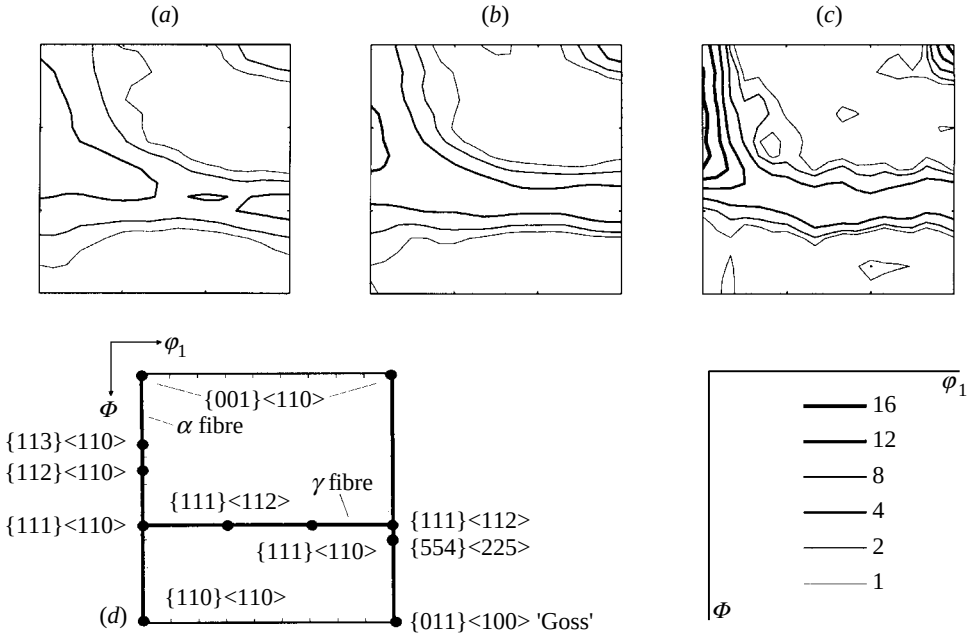

Figure 1. ODF sections ($\phi_2 = 45°$) for low-carbon steel cold rolled (*a*) 50%, (*b*) 74%, (*c*) 95% and (*d*) key to the main components. Experimental data from Schläfer & Bunge (1974).

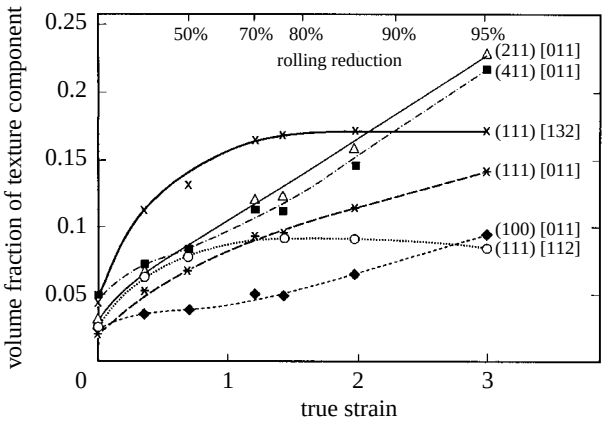

Figure 2. Volume fractions of material within 10° of the given orientations in cold-rolled low-carbon steel. Based on data of Schläfer & Bunge (1974).

tion. The former contains components such as $\{100\}\langle 011\rangle$ and $\{211\}\langle 011\rangle$ as well as $\{111\}\langle 011\rangle$, which also belongs to the γ-fibre as does $\{111\}\langle 112\rangle$.

Evolution of the rolling texture is more easily seen by integrating the density in a spherical volume of orientation space around various ideal orientations. This leads to a value of the volume fraction of material lying within a certain range, here chosen to be 10°. Figure 2 shows how the volume fraction for various important components increases with strain during cold rolling. The α-fibre components strengthen continuously, whereas the $\{111\}\langle 112\rangle$ component and other parts of the γ-fibre increase up

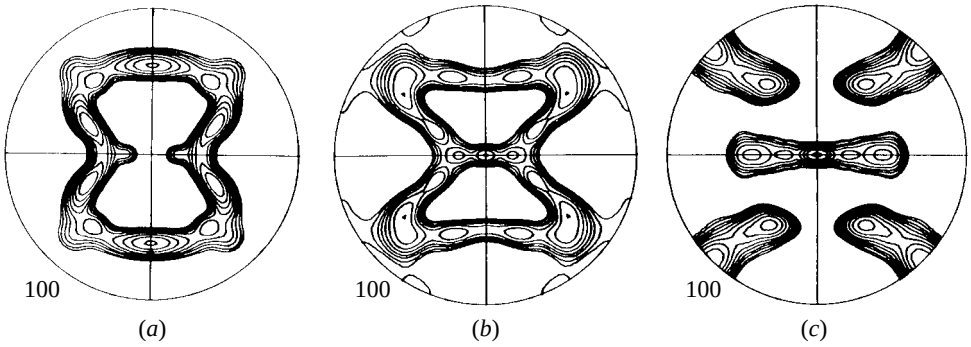

Figure 3. Calculated {100} pole figures for BCC ferrite on the bases of (*a*) the fully constrained Taylor model; (*b*) the relaxed constraint 'lath' model; and (*c*) the relaxed constraint 'pancake' model. From van Houtte (1984).

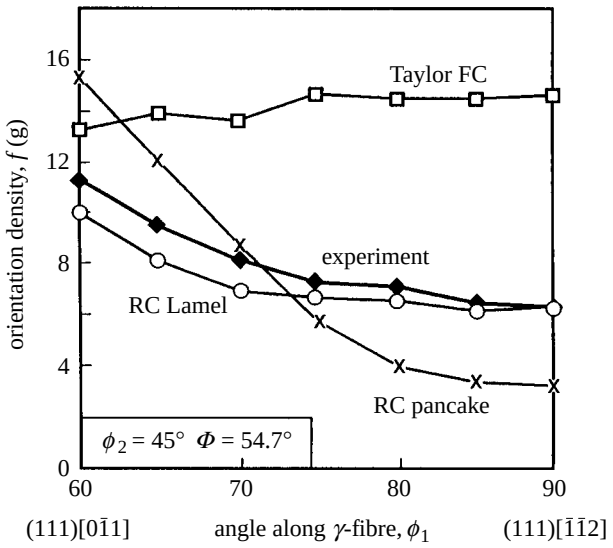

Figure 4. Experimental and various calculated orientation densities along the γ-fibre for cold-rolled steel. From van Houtte *et al*. (1999).

to *ca.* 70% reduction, but thereafter remain almost constant. In the original paper, the relative weakness of the $\{111\}\langle 112\rangle$ orientation at high strains was attributed to re-orientation by deformation twinning. No metallographic evidence has been found for twinning, however, and other explanations have now been provided as discussed below. This demonstrates the dangers that exist in trying to identify deformation mechanisms solely on the basis of resulting textures.

Attempts to model the rolling texture of ferrite have met with mixed success. The fully constrained Taylor model (Dillamore & Katoh 1974; van Houtte 1984) predicts the components $\{211\}\langle 011\rangle$ and $\{11, 11, 8\}\langle 4, 4, 11\rangle$, the latter being 8° from the simpler, and often reported, orientation $\{111\}\langle 112\rangle$. If the constraints are relaxed, permitting shears to occur in the rolling plane (lath and pancake models), other components of the α-fibre such as $\{100\}\langle 011\rangle$ and $\{111\}\langle 011\rangle$ are predicted to develop

(figure 3). A transition from full constraint at low strains when the grains are nearly equiaxed to progressively relaxed constraint as the deformation and grain flattening proceeds can, therefore, rationalize the stagnation of the $\{111\}\langle 112\rangle$ texture and the continued strong evolution of the α-fibre. Recent work by van Houtte *et al.* (1999) has considerably improved the predictions of relaxed constraint modelling by concentrating on pair-wise interactions between grains, in which the evolution of grain shape with strain is also included. This so called 'Lamel' model describes the variation of orientation density along the γ-fibre well, as can be seen from the comparison of experimental measurements with different model predictions shown in figure 4.

A problem with the models is that they tend to predict much sharper textures than are observed in practice. This is probably due to deviations in strain state between different grains, which may occur systematically (but outside the range assumed in the relaxed constraint models) or non-systematically depending on the local environment of each individual grain. Some examples of these phenomena will be included later.

3. Deformation substructures and stored energies

In cold-rolled steels, the substructure is strongly correlated with the orientation of the deformed grain. This was first remarked on by Dillamore *et al.* (1967) who measured subgrain diameters and misorientations in 70% cold-rolled iron using transmission electron microscopy (TEM) for different texture components along the α-fibre (figure 5). The stored energies in figure 5 have been recalculated based on the original measurements together with later more complete values of sub-boundary energy due to Avraamov *et al.* (1973). These measurements were rather crude, being based on foils taken from the rolling plane section of the sheet, which obscures much of the detail but, nevertheless, established a pattern that has been amply confirmed. The $\{100\}\langle 011\rangle$ component contains the coarsest structure with the lowest misorientations and, accordingly, contains the lowest stored energy of deformation. The opposite extreme is found in $\{011\}\langle 011\rangle$, which is only a very minor component of the texture. Of the major components, it is the γ-fibre that represents the largest stored energy of deformation. These TEM results are supported by X-ray line broadening results of Every & Hatherly (1974) and Matsuo *et al.* (1971), where measurements were made on reflections from different crystal planes lying parallel to the cold-rolled steel sheet, and also by the neutron diffraction measurements of Rajmohan *et al.* (1996). Various analyses of the diffraction data have been applied but all generally lead to the same conclusion: that the volumetric stored energy for different orientations V_{hkl} are ranked in the sequence:

$$V_{110} > V_{111} > V_{211} > V_{100}.$$

Figure 5 compares results obtained by Fourier analysis of X-ray diffraction peaks with those from TEM observations, and it can be seen that the agreement is quite good considering that the materials, as well as the experimental methods and analyses, were all different. Also plotted in figure 5 are the Taylor M values for the same orientations along the α-fibre. These values are based on pencil glide with $\langle 111\rangle$ slip directions, which is believed to be the most appropriate for BCC ferrite, although the variation is similar if planar glide on $\{110\}$ is assumed instead. One interpretation of the Taylor factor is that it represents, for different crystal orientations, the

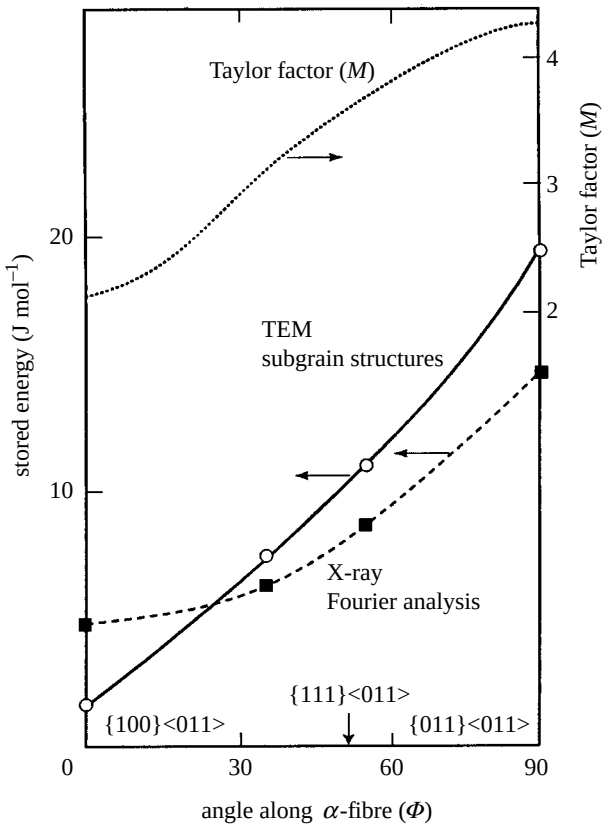

Figure 5. Stored energies of deformation for different orientations in the α-fibre of cold-rolled iron and steel. TEM results from Dillamore *et al*. (1967) and X-ray Fourier analysis from Every & Hatherly (1974). Also shown is the variation of the Taylor factor, M.

total amount of slip activity; that is to say the product of dislocation density and slip length. If the number of locked-in dislocations increases monotonically with the slip activity, then the stored energy of deformation would be expected to show a correlation with a Taylor factor of the type seen in figure 5.

Variations in substructure between grains of different orientations (texture components) have been recognized in many metallographic studies. Optical microscopy on polished and etched specimens shows different degrees of attack, such that some grains appear dark and others light. Dillamore & Hutchinson (1974) showed by use of an etch-pitting technique that the dark heavily etched grains were predominantly {111} oriented, while the light-coloured grains were always {100}–{211} oriented. Examination of lightly annealed samples revealed that early nucleation of recrystallization was almost entirely restricted to the {111} oriented grains (see, for example, figure 6), and that the new grains also belonged to the {111}, γ-fibre, components. A reasonable interpretation of this was that *in situ* nucleation of recrystallized grains takes place most rapidly within regions of high-stored energy.

Other studies by Kern (1984) using optical microscopy have confirmed and ex-

Figure 6. Optical micrograph showing lightly annealed cold-rolled steel. Nucleation of recrystallization occurs preferentially in the dark etching grains that are mostly {111} oriented.

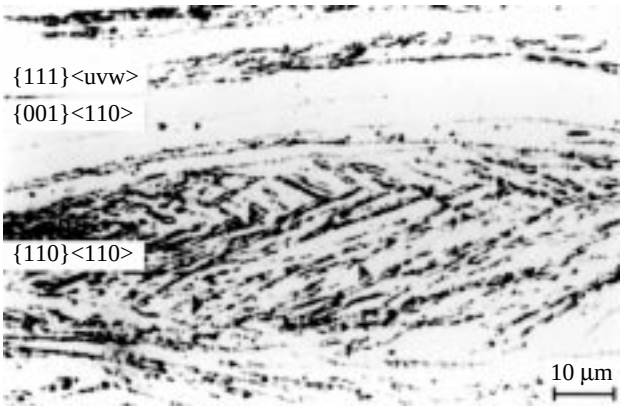

Figure 7. Example of a hard $\{011\}\langle 011\rangle$ oriented grain in cold-rolled steel containing a 'splintered' or 'fish-bone' microstructure (Vanderscheuren *et al*. 1996).

tended the above observation. By heat-tint-etching there were seen to be three general types of microstructures in cold-rolled iron of different purities. 'Smooth' regions without fine structure consisted of $\{100\}\langle 011\rangle$ to $\{211\}\langle 011\rangle$ orientations, and these regions sometimes merged gradually into one another suggesting gradual long-range curvatures. 'Grooved' regions were dominated by $\{111\}\langle 112\rangle$ orientations but also by other components of the γ-fibre, spreading as far as the $\{111\}\langle 011\rangle$. The third type of structure, sometimes described as 'splintered', occurred in transition zones and sometimes alone. The crystal orientation within these was widely spread and could not be identified with the technique available. A probable explanation of at least some of the 'splintered' grains was given by Vanderscheuren *et al*. (1996) who combined optical microscopy with SEM and the electron back-scattering patterns (EBSP) technique. Certain grains having a pronounced 'fish-bone' structure (figure 7) belonged nominally to the $\{011\}\langle 011\rangle$ orientation but contained large internal misorientations consistent with the high-stored-energy description given earlier. Such

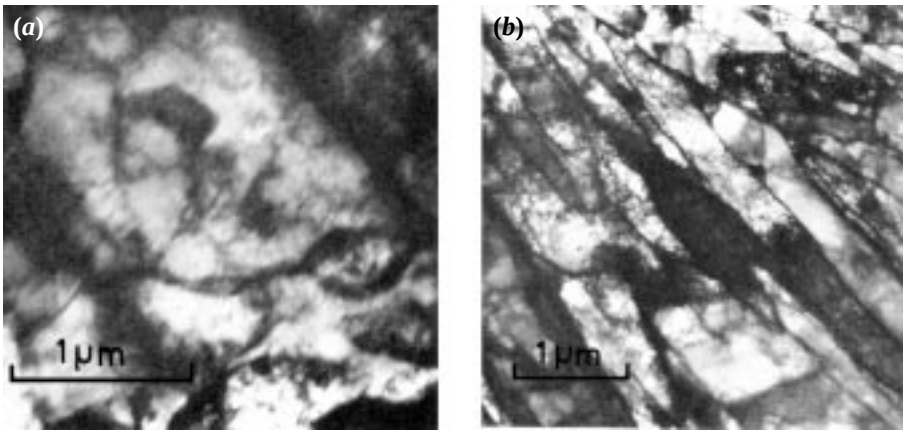

Figure 8. TEM micrographs from the long transverse section of cold-rolled steel (*a*) typical α-fibre grain, (*b*) typical γ-fibre grain. From Every & Hatherly (1974).

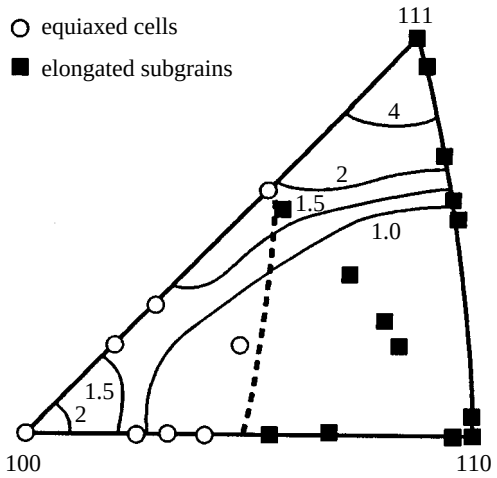

Figure 9. Unit triangle showing the occurrence of different types of dislocation substructure for different grain orientations in 70% cold-rolled steel superimposed on an ND inverse pole figure. Data from Every & Hatherly (1974).

regions were relatively uncommon but produced copious recrystallization nuclei on annealing, having orientations near $\{122\}\langle 011\rangle$ and in the γ-fibre.

Other metallographic techniques confirm that there are systematic differences in substructures between grains of different orientations in cold-rolled steel. Every & Hatherly (1974), using TEM on transverse sections of the sheet, showed that the α-fibre grains in the range $\{100\}$ to $\{211\}$ were characterized by equiaxed cells with walls consisting of dislocation tangles, such as those shown in figure 8*a*. Misorientations across these structures tend to be small, *ca.* 3°, and generally not cumulative. Such regions show little tendency to recrystallize spontaneously on annealing. It is possible that these diffuse cell structures are not persistent but dissolve up during each pass of deformation and subsequently relax into new cell structures on unloading.

The fine structure of γ-fibre grains consists mainly of elongated subgrains with quite well-defined boundaries, mainly lying parallel to the rolling plane, figure 8*b*. These are the features described as lamellar boundaries in the terminology of Hansen & Hughes (1995), and are frequently intersected by bands of elongated subgrains at an angle of some 30° to the main family of lamellae. Such intersecting slip structures resemble the features described as *S*-bands in aluminium, copper and nickel. Misorientations are significantly larger within the lamellar substructures of the {111} grains, frequently reaching 10° or more, and there is a tendency for the subgrain orientations to be rotated around the sheet normal direction, i.e. spread along the γ-fibre. Occurrence of the two types of substructures has been related to the grain orientation in a normal direction inverse pole figure representation for rolled as well as recovered structures in steels, as shown in figure 9. Equiaxed cells exist up to *ca.* 30° from {100}, principally in the α-fibre grains to about $\{211\}\langle 011\rangle$. Along the γ-fibre, the substructure typically comprises lamellar subgrains. The pattern of behaviour is also evident in other orientations, but those are only weakly represented in the texture and so are of less importance statistically.

4. Deformation heterogeneities

When trying to rationalize the structures and textures of deformed steel, it soon becomes apparent that heterogeneity exists at several different levels. The rolling texture itself is incompatible with homogeneous Taylor-type deformation, and seems to imply that different components (grains) deviate systematically from ideal plane strain with shears in the rolling and transverse directions, especially at high deformations where the grains have become significantly flattened and so can accommodate such effects in the way described by Honeff & Mecking (1981).

In addition to those systematic strain heterogeneities there are interactions that depend on the proclivity of individual grains in the specific environment of their neighbours. Especially at low to medium strains, those grains having high Taylor factors and, therefore, higher flow stresses than others will tend to resist deformation, whereas those with low Taylor factors will undergo more. A nice example of this can be seen in figure 7, where a hard $\{110\}\langle 110\rangle$ grain ($M = 4.33$) is adjacent to a soft $\{001\}\langle 110\rangle$ grain ($M = 2.12$). The hard grain tends to resist deformation and has an aspect ratio of about 5, as compared with the expected value of 22 based on fully homogeneous deformation (at 79% rolling reduction). At the same time, the softer $\{001\}\langle 110\rangle$ grain has had to bend around this rather hard 'inclusion', and its orientation will be spread, leading to a weakening of the texture. Such effects are now capable of being modelled using crystallographic finite-element models (Dawson *et al.* 1994; Bate, this issue). They may be expected to contribute to the observed spread of orientation density around the ideal components. In particular, the softer α-fibre grains are likely to show a greater dispersion of texture for this reason as discussed by van Houtte *et al.* (1999).

A further level of heterogeneity, and probably the most practically important in sheet steels, occurs within individual deformed grains. Slip, by virtue of its discrete nature, can never be homogeneous at the smallest level, but it may be more or less heterogeneous. An experiment to investigate this was carried out by Ryde & Hutchinson (unpublished work at the Swedish Institute for Metals Research) using an extra-low-carbon steel sheet (virtually pure iron) having an initial grain size of

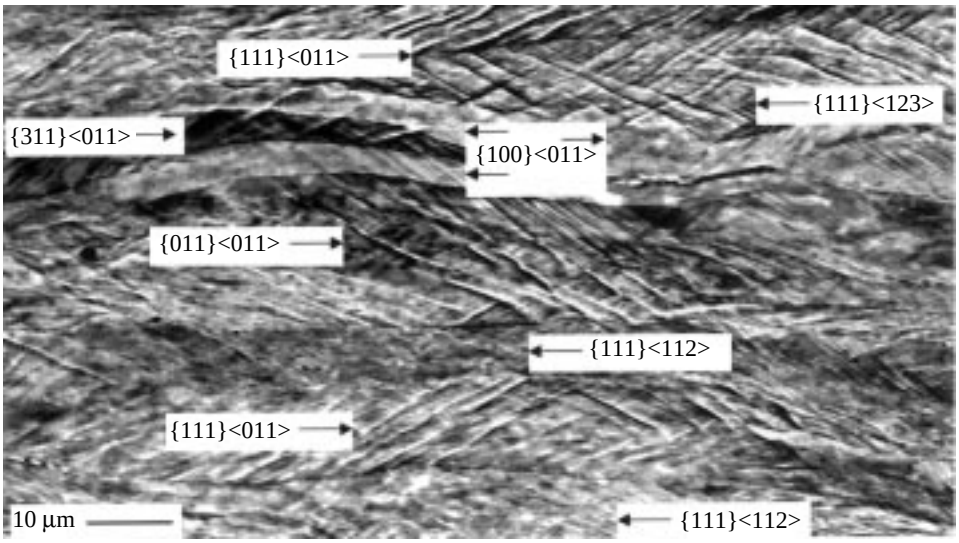

Figure 10. Slip steps on the polished long transverse section of 75% cold-rolled extra-low-carbon steel following a small final rolling deformation. Scanning electron micrograph with grain orientations determined by EBSP.

30 µm. This was cold rolled to 75% reduction and a long edge section was ground flat and electropolished. A second small rolling reduction was carefully applied giving a final total reduction of 77%, and the polished surface was then examined by SEM. The pattern of slip lines observed as surface topography was related to the individual grain orientations using the EBSP technique, as shown in the annotated micrograph in figure 10. Grains in the α-fibre close to $\{100\}\langle 011\rangle$ reveal no trace of slip lines in most cases. The deformation is evidently homogeneous on a very fine scale. The slip becomes coarser for orientations further along the α-fibre, such as $\{311\}\langle 011\rangle$, and especially coarse at $\{111\}\langle 011\rangle$ and $\{011\}\langle 011\rangle$. Generally, the coarseness of slip decreases with increasing angle ϕ_1 along the γ-fibre, becoming moderately fine within the grain orientation $\{111\}\langle 112\rangle$.

These observations show significant similarities with the variations of stored energy described above. They lead to a viewpoint that cell size and misorientation are not fundamentally determined by the Taylor factors of the grains, but rather by their tendency for heterogeneous deformation or slip localization. Naturally, these effects may be related to one another. A grain with a small Taylor factor for plane-strain deformation cannot make a saving of energy by concentrating the deformation into localized shears. On the other hand, shear-band formation may involve a lower total deformation energy if the grain orientation is such as to require a high stress for flow in homogeneous plane strain, as discussed by Gil Sevillano *et al*. (1980). In general terms, it appears that intragranular heterogeneities in steel tend to concentrate in grains of the hard γ-fibre orientations, whereas non-systematic intergranular strain heterogeneities affect mainly grains of the softer α-fibre orientations.

In some situations, the tendency for localized shearing in bands may be drastically increased in ferrite (Furubayashi 1969; Ushioda *et al*. 1981; Ushioda & Hutchinson 1989). This happens if the grain size is large or if there is a relatively high interstitial content of carbon or nitrogen and, in particular, under conditions of dynamic strain

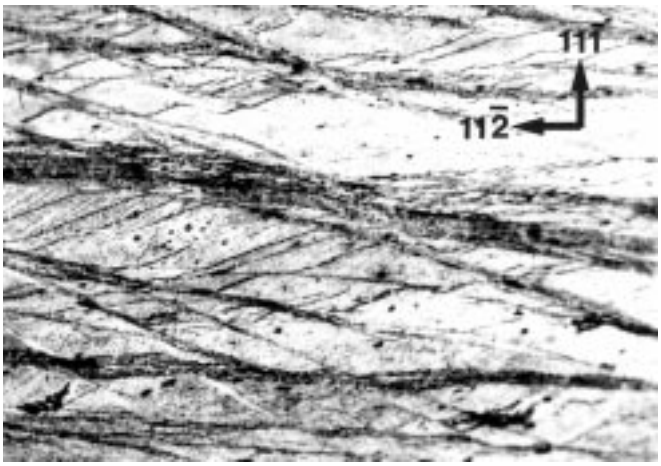

Figure 11. Shear bands in a cold-rolled single crystal of 3% silicon iron having the orientation (111)[11$\bar{2}$]. From Haratani *et al.* (1984).

ageing (DSA). The negative strain-rate sensitivity of flow stress in DSA encourages any tendency for local shearing with a concomitant higher strain rate. Grains of the $\{111\}\langle 112\rangle$ orientation are particularly susceptible to coarse shear banding, where very high strains of several hundred per cent are localized (figure 11). The shear directions within these bands do not correspond to simple crystallographic slip directions and there are large associated crystal rotations that have been rationalized in terms of poly-slip by Haratani *et al.* (1984). The effect of shear banding when it occurs is to weaken somewhat the rolling deformation texture of the steel. On subsequent annealing, profuse nucleation of recrystallization takes place in the highly strained shear-band structures, which leads to new grains and final textures having the Goss orientation.

While the effect of negative strain-rate sensitivity on shear localization has been recognized for many years, the contrary effect of positive strain-rate sensitivity on texture formation is only now becoming appreciated. Theoretical treatments of deformation texture by Asaro & Needleman (1985) suggested that positive-rate sensitivity should reduce the rate of crystal rotation and, accordingly, give rise to a weakening of the texture. This is precisely the opposite of what is usually observed in practice. For example, aluminium alloys have sharper textures after hot rolling at temperatures where the strain-rate sensitivity index, m, is significantly positive than at room temperature, where $m \sim 0$. The difference in texture is accompanied by a distinctly more homogeneous laminar microstructure at the higher temperature (Hutchinson & Ekström 1990).

Some very interesting results of Barnett & Jonas (1997) have recently demonstrated the significance of strain-rate sensitivity in warm rolling of ferrite, a process that is finding growing industrial application. It was shown that the presence of interstitial atoms (notably carbon) in steels at temperatures above the DSA range can provide a viscous drag on dislocation movement such that the strain-rate dependence of flow stress becomes substantially positive. Interstitial-free (IF) steels, where the impurity elements are combined in stable particles (TiN, TiC), do not show this behaviour. In figure 12, the strain-rate sensitivity index is plotted for two steels,

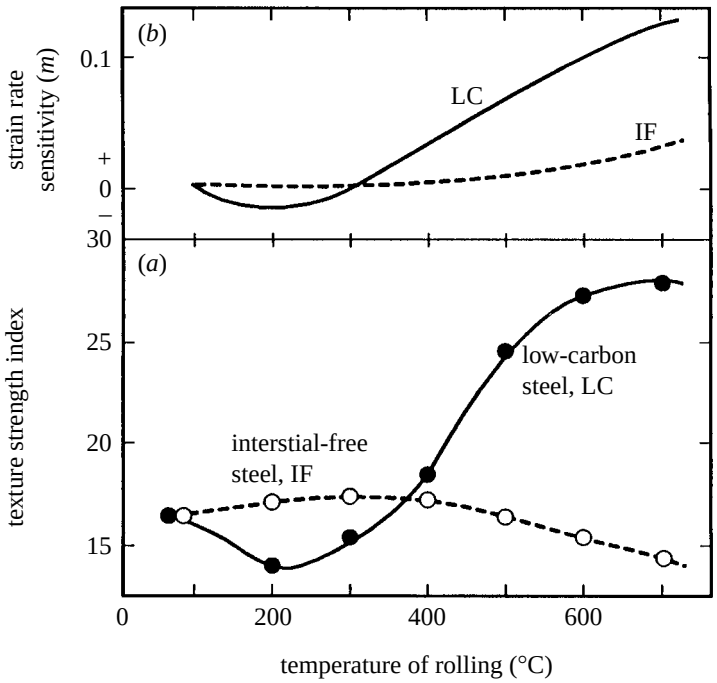

Figure 12. Effect of ferrite rolling temperature for interstitial-free (IF) and low-carbon (LC) steels on (*a*) strength of the deformation texture; and (*b*) strain-rate sensitivity index, m. From Barnett & Jonas (1997).

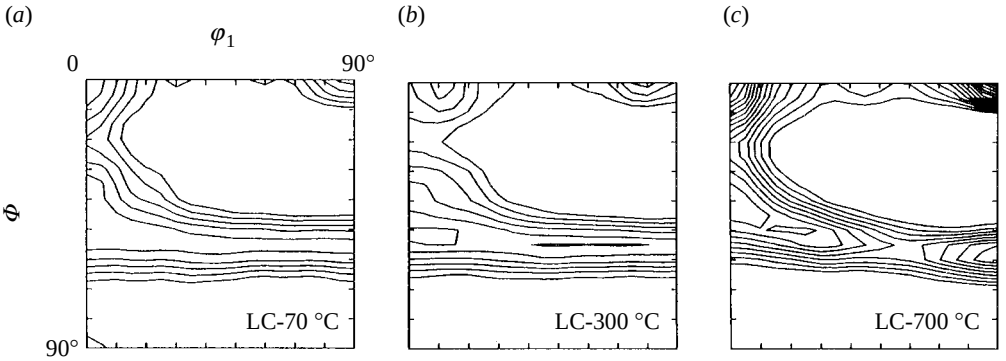

Figure 13. ODF sections ($\phi_2 = 45°$) for low-carbon steel rolled 65% at (*a*) room temperature, (*b*) 300 °C, and (*c*) 700 °C. From Barnett & Jonas (1997).

with and without interstitial carbon, as a function of deformation temperature. Also shown in figure 12 are measures of the texture sharpness, defined as the sum of three major components in the α- and γ-fibres. It is evident that for the IF steel, m is close to zero at all temperatures and the strength of the deformation texture varies only slightly. The interstitial-containing low-carbon steel, on the other hand, has a region of slightly weakened texture in the vicinity of 300 °C, where m becomes negative, but then produces very much sharper textures at temperatures above 400 °C, where m is

markedly positive. ODF sections for the low-carbon steel at three different temperatures are reproduced in figure 13. For rolling at 300 °C in the DSA range, the texture is slightly weaker than at room temperature, notably in the vicinity of $\{111\}\langle 112\rangle$, which is the orientation that is prone to shear banding, as discussed above. However, at 700 °C, the texture generally becomes much sharper and is especially strong just in the components close to $\{111\}\langle 112\rangle$.

Later work by Barnett (1998) has confirmed by microscopical examination that the pattern of deformation becomes much more homogeneous in the range of positive strain-rate sensitivity. In particular, concentrations of local slip within grains of the γ-fibre, such as those shown in figure 10, were virtually eliminated in steel rolled at 700 °C. The substructures in these γ-fibre grains consisted of diffuse cells with misorientations of only 1–2°, as compared to a mean misorientation of 8° for subgrains in the same steel rolled at room temperature. It was also shown that the preferential nucleation of recrystallized γ-fibre grains during annealing was eliminated after warm rolling, leading to a technologically inferior texture in the final low-carbon steel product.

Evidently, a modestly positive strain-rate sensitivity with $m \sim 0.1$ provides for a more homogeneous deformation environment, where lattice rotations resulting from slip take place in a more consistent manner than is otherwise the case, so leading to formation of a sharper deformation texture. To some extent, this derives from the observed reduction in intragranular slip heterogeneity. The increased uniformity of deformation between grains is also likely to be important. Some calculations have been carried out by Bate (1998, personal communication) using the crystal-plasticity-based finite-element modelling approach to investigate the possible role of strain-rate sensitivity. These confirmed that increasing the factor m in the range 0–0.2 should lead to texture sharpening as a result of increasing homogeneity of deformation. Only at higher values of m did the predicted textures become weaker due to reduction in the rate of crystal rotation. With moderately positive strain-rate sensitivity, the material behaviour appears to approach Taylor's description of polycrystalline plasticity more closely. The warm rolling texture in figure 13*c* is, in fact, very similar to calculated textures for fully constrained plane-strain deformation by Dillamore & Katoh (1974), having maxima close to the $\{211\}\langle 011\rangle$ and $\{111\}\langle 112\rangle$ orientations. Nevertheless, some relaxation of constraints as in the 'pancake' or 'Lamel' models of van Houtte *et al*. (1984, 1999) may be invoked to explain the presence of a significant $\{100\}\langle 011\rangle$ component and the spread towards $\{111\}\langle 011\rangle$.

The author is grateful to Mathew Barnett, Paul van Houtte and Dirk Vanderscheuren for making available material for this review. The author also thanks Lena Ryde and Dorota Artymowicz for assistance, and Peter Bate for many helpful discussions and for carrying out CPFEM calculations regarding the effect of strain-rate sensitivity.

References

Asaro, R. J. & Needleman, A. 1985 Texture development and strain hardening in rate dependent polycrystals. *Acta. Metall.* **33**, 923–954.

Avraamov, Yu. S., Gvozdev, A. G. & Kutsak, V. M. 1973 Orientation dependence of grain boundary energy of Si iron. *Phys. Met. Metallog.* **36**, 198–201.

Barnett, M. R. 1998 Role of in-grain shear bands in the nucleation of ⟨111⟩ ND recrystallisation textures in warm rolled steel. *ISIJ Int.* **38**, 78–85.

Barnett, M. R. & Jonas, J. J. 1997 Influence of ferrite rolling temperature on microstructure and texture in deformed low C and IF steels. *ISIJ Int.* **37**, 697–705.

Dawson, P. R., Beaudoin, A. J. & Mathur, K. K. 1994 Finite element modelling of polycrystalline solids. *Mat. Sci. Forum* **157–162**, 1703–1712.

Dillamore, I. L. & Hutchinson, W. B. 1974 The control of grain size and orientation in sheet steel. *Trans. ISIJ* **11**, 877–883.

Dillamore, I. L. & Katoh, H. 1974 A comparison of the observed and predicted deformation textures in cubic metals. *Metal Sci. J.* **8**, 21–25.

Dillamore, I. L., Smith, C. J. E. & Watson, T. W. 1967 Oriented nucleation in the formation of annealing textures in iron. *Metal Sci. J.* **1**, 49–54.

Every, R. L. & Hatherly, M. 1974 Oriented nucleation in low carbon steels. *Texture* **4**, 183–194.

Furubayashi, E. 1969 Origin of the recrystallised grains with preferred orientations in cold rolled Fe–3%Si. *Trans. ISIJ.* **9**, 222–238.

Gil Sevillano, J., van Houtte, P. & Aernoudt, E. 1980 Large strain work hardening and textures. *Progr. Mater. Sci.* **25**, 69–412.

Hansen, N. & Hughes, D. A. 1995 Analysis of large dislocation populations in deformed metals. *Phys. Stat. Sol.* **149**, 155–172.

Haratani, T., Hutchinson, W. B., Dillamore, I. L. & Bate, P. 1984 The contribution of shear banding to the origin of Goss texture in silicon iron. *Metal Sci.* **18**, 57–65.

Heckler, A. J. & Granzow, W. G. 1970 Crystallite orientation distribution analysis of the cold rolled and recrystallised textures in low-carbon steels. *Met. Trans.* **1**, 2089–2094.

Honeff, H. & Mecking, H. 1981 Analysis of the deformation texture at different rolling conditions. In *Proc. ICOTOM-6* (ed. S. Nagashima), pp. 347–355. Tokyo: ISIJ.

Hutchinson, W. B. & Ekström, H.-E. 1990 Control of annealing texture and earing in non-hardenable aluminium alloys. *Mater. Sci. Technol.* **6**, 1103–1111.

Inagaki, H. 1987 Stable end orientations in the rolling textures of polycrystalline iron. *Z. Metallkunde* **78**, 431–439.

Inagaki, H. 1994 Fundamental aspect of texture formation in low carbon steel. *ISIJ Int.* **34**, 313–321.

Jago, R. A. & Hansen, N. 1986 Grain size effects in the deformation of polycrystalline iron. *Acta Metall.* **34**, 1711–1720.

Kern, R. 1984 Application of metallographic methods for investigation of orientations in cold rolled and recrystallised iron. *Pract. Metallography* **21**, 273–293.

Langford, G. & Cohen, M. 1969 Strain hardening of iron by severe plastic deformation. *Trans. ASM* **62**, 623–638.

Matsuo, M., Hayami, S. & Nagashima, S. 1971 Study of recrystallisation texture formation in cold rolled iron sheets with X-ray diffraction techniques. In *Advances in X-ray analysis*, vol. 14, pp. 214–230. New York: Plenum.

Rajmohan, N., Hayakawa, Y., Szpunar, J. A. & Root, J. H. 1996 Neutron diffraction method for stored energy measurement in interstitial free steel. *Acta Mater.* **45**, 2485–2494.

Roven, H. J. & Nes, E. 1984 Structures and properties of heavily cold rolled iron and high strength low alloy and low carbon steels. *Metal Sci.* **18**, 515–520.

Schläfer, D. & Bunge, H.-J. 1974 The development of rolling texture in iron determined by neutron-diffraction. *Texture* **1**, 157–171.

Ushioda, K. & Hutchinson, W. B. 1989 Role of shear bands in annealing texture formation in 3%Si–Fe (111)[112] single crystals. *ISIJ Int.* **29**, 862–867.

Ushioda, K., Ohsone, H. & Abe, M. 1981 Recrystallisation textures after rolling under the condition of dynamic strain ageing. In *Proc. ICOTOM-6*, pp. 829–838. Tokyo: ISIJ.

Vanderscheuren, D., Yoshinaga, N. & Koyama, K. 1996 Recrystallisation of Ti IF steel investigated with electron back-scattering patterns (EBSP). *ISIJ Int.* **36**, 1046–1054.

PHILOSOPHICAL TRANSACTIONS OF THE ROYAL SOCIETY A MATHEMATICAL, PHYSICAL & ENGINEERING SCIENCES

Van Houtte 1984 Some recent developments in the theories for deformation texture prediction. In *Proc. ICOTOM-7, Holland* (ed. C. M. Brakman), pp. 7–23.

Van Houtte, P., Delannay, L. & Samajdar, I. 1999 Quantitative prediction of cold rolling textures in low-carbon steel by means of the LAMEL model. *Textures Microstruct.* **31**, 109–149.

Von Schlippenbach, U., Emren, F. & Lücke, K. 1986 Investigation of the development of the cold rolling texture in deep-drawing steels by ODF-analysis. *Acta Metall.* **34**, 1289–1301.

Discussion

N. Hansen (*Materials Research Department, Risø National Laboratory, Roskilde, Denmark*). In discussing the relationship between texture and microstructure, Professor Hutchinson showed ill-defined structures in regions at alpha-fibre orientation. Can the cause of this structure be explained by recovery as proposed by him and Riddha on microstructure formation in FCC grains of cube orientation?

B. Hutchinson. The mechanism we proposed was specific to the cube orientation in FCC metals where recovery of dislocations was thought to be especially rapid due to the occurrence of dislocation populations having only orthogonal Burgers vectors. In BCC steels where the glide directions are $\langle 111 \rangle$, this situation cannot arise, so I suppose that the alpha-fibre substructures should be explained in other terms.

P. van Houtte (*Department MTM, K.U. Leuven, Belgium*). Professor Hutchinson said that in deformed steel sheet, the grains of the gamma-fibre show a deformation pattern (fishbone pattern) due to heterogeneous strain, whereas the grains of the alpha-fibre do not. He then expressed the opinion that the reason for this could be that the grains of the gamma-fibre have a high Taylor factor, whereas those of the alpha-fibre have a low Taylor factor.

Could the reason not rather be that the deformation of the soft grains (alpha-fibre) is so much disturbed by heterogeneity of plastic flow that a fishbone pattern never has the chance to become visible?

B. Hutchinson. I do not believe so because one almost never sees such patterns in alpha-grains, even when they seem to be in regions of reasonable homogeneous strain.

D. Juul Jensen (*Materials Research Department, Risø National Laboratory, Roskilde, Denmark*). My question concerns the etch effects seen in optical micrographs. Professor Hutchinson said the 'colours' seen in the micrographs reflect the orientation of the grains, but do they reflect something more. He showed a deformation microstructure with white and dark grains, each group representing different orientations. In this structure nuclei appeared to develop preferentially in dark coloured deformed grains and he reported that these nuclei have orientations close to the deformation orientations in the dark regions (maybe with some rotation), but the nuclei were white, not dark.

B. Hutchinson. Dr Juul Jensen is quite correct. It is not the orientation of the specimen surface that controls the etching response but rather the dislocation substructure density. Thus the gamma-fibre grains appear dark in the deformed condition where they are heavily dislocated, but almost white when recrystallized and so nearly free from dislocations.

PHILOSOPHICAL TRANSACTIONS OF THE ROYAL SOCIETY A MATHEMATICAL, PHYSICAL & ENGINEERING SCIENCES